

A single methyl group drastically changes urea's hydration dynamics

Cite as: J. Chem. Phys. **156**, 164504 (2022); <https://doi.org/10.1063/5.0085461>

Submitted: 17 January 2022 • Accepted: 07 April 2022 • Accepted Manuscript Online: 08 April 2022 •

Published Online: 27 April 2022

 Bogdan A. Marekha and  Johannes Hunger

COLLECTIONS

Paper published as part of the special topic on [Time-resolved Vibrational Spectroscopy](#)



View Online



Export Citation



CrossMark

ARTICLES YOU MAY BE INTERESTED IN

[Solvation shell thermodynamics of extended hydrophobic solutes in mixed solvents](#)

The Journal of Chemical Physics **156**, 164901 (2022); <https://doi.org/10.1063/5.0090646>

[Progress and perspectives in single-molecule optical spectroscopy](#)

The Journal of Chemical Physics **156**, 160903 (2022); <https://doi.org/10.1063/5.0087003>

[Stretchy and disordered: Toward understanding fracture in soft network materials via mesoscopic computer simulations](#)

The Journal of Chemical Physics **156**, 160901 (2022); <https://doi.org/10.1063/5.0081316>

The Journal of Chemical Physics **Special Topics** Open for Submissions

[Learn More](#)

A single methyl group drastically changes urea's hydration dynamics

Cite as: J. Chem. Phys. 156, 164504 (2022); doi: 10.1063/5.0085461

Submitted: 17 January 2022 • Accepted: 7 April 2022 •

Published Online: 27 April 2022



View Online



Export Citation



CrossMark

Bogdan A. Marekha^{a)}  and Johannes Hunger^{b)} 

AFFILIATIONS

Max Planck Institute for Polymer Research, Ackermannweg 10, 55128 Mainz, Germany

Note: This paper is part of the JCP Special Topic on Time-Resolved Vibrational Spectroscopy.

^{a)} **Present address:** Max Planck Institute for Medical Research, Jahnstraße 29, 69120 Heidelberg, Germany.

^{b)} **Author to whom correspondence should be addressed:** hunger@mpip-mainz.mpg.de. Telephone: +49 6131 379 765

ABSTRACT

The amphiphilicity and denaturation efficiency of urea can be tuned via alkylation. Although the interaction of alkylureas with water and proteins has been studied in detail, hydration of 1-methylurea has remained elusive, precluding the isolation of the effect of an individual methyl group. Here, we study water dynamics in the hydration shell of 1-methylurea (1-MU) using infrared absorption and ultrafast infrared spectroscopies. We find that 1-MU hardly affects the hydrogen-bond distribution of water as probed by the OD stretching vibration of HOD molecules. Polarization resolved infrared pump-probe experiments reveal that 1-MU slows down the rotational dynamics of up to 3 water molecules in its hydration shell. A comparison to earlier results for other alkylureas suggests that further alkylation does not necessarily slow down the rotational dynamics of additional water molecules. Two-dimensional infrared experiments show that 1-MU markedly slows down the hydrogen-bond fluctuation dynamics of water, yet similar to what has been found for urea and dimethylureas. Remarkably, (alkyl-)ureas that share a similar effect on water's hydrogen-bond fluctuation dynamics have a similar (modest) protein denaturation tendency. As such, not only the hydrophobicity but also hydration of hydrophilic fragments of alkylureas may be relevant to explain their function toward biomolecules.

© 2022 Author(s). All article content, except where otherwise noted, is licensed under a Creative Commons Attribution (CC BY) license (<http://creativecommons.org/licenses/by/4.0/>). <https://doi.org/10.1063/5.0085461>

INTRODUCTION

The interaction and dynamics of water around amphiphilic solutes are at the heart of various biologically and technologically relevant phenomena such as self-assembly, solubilization, osmotic protection, and protein denaturation.^{1–6} To understand the underlying molecular-level details of such effects of osmolytes on solutes, urea and alkylureas are an ideal test system, as the amphiphilicity can be tuned by varying the number and position of the hydrophobic alkyl groups. Thus, the effect of amphiphilicity on the hydrating water molecules can be systematically studied.^{3,7–13} In addition to the effect on hydrating water molecules, both the degree of alkylation and the alkylation pattern profoundly alter the destabilizing effect of substituted ureas on biomolecules.^{4,14,15} In general, the tendency of alkylureas to destabilize biomolecules increases with increasing alkyl substitution,^{4,12,14–17} despite direct urea-biomolecule contacts can be reduced upon alkyl substitution.^{18,19} These findings have hinted at an indirect mechanism of (alkyl-)urea induced effects on the protein structure. In line with that, the hydrogen-bond donor number of urea/water mixtures has been shown to scale with the

destabilization of intermolecular peptide bonds.⁴ However, the substitution of urea's protons with a single methyl group 1-methylurea (1-MU) may even reduce the destabilizing effect of urea.^{14,17} Together, these findings suggest that the subtle interplay between hydrophobic and hydrophilic interactions for substituted ureas, mediated by the hydrogen-bonded structure of urea-water mixtures, is decisive for their effect on biomolecules.

Due to the importance of the hydration of alkylureas for their function, the interaction of different ureas with water has been studied in great detail.^{3,8–11,20–23} Yet, competing effects such as conformational flexibility or clustering of alkylureas prevent an intuitive understanding of alkylureas' effects on water and solutes.¹⁰ For instance, the enthalpy of solvation scales linearly with the length of the alkyl substituents, yet branching of the alkyl substituents or distribution of the substituents makes solvation energetically less favorable.^{8,24} Hydration dynamics can be even more complex.^{25–27} Similar to the subtle influence of the substitution pattern on the hydration energetics, we have recently shown that also the dynamics of water molecules hydrating alkylureas with two methyl(ene) groups vary markedly.⁹ In contrast to the negligible effect of urea

itself on water dynamics,^{28,29} the temporal variation of hydrogen-bond strengths, as measured by the spectral diffusion of the stretching vibration $\nu(\text{OD})$ of the vibrational probe HOD, is slowed down by 1,1-dimethylurea (1,1-DMU) and 1,3-dimethylurea (1,3-DMU), but 1-ethylurea (1-EU) hardly affects these dynamics. This impact of the substitution pattern on hydrogen-bond dynamics suggested a more pronounced exposure of the hydrogen bonding groups of 1,1-DMU and 1,3-DMU, as compared to 1-EU. Conversely, 1,3-DMU, bearing two spatially separated methyl groups, markedly slows down the rotational dynamics of the water, which require breaking and reformation of hydrogen bonds. Thus, the effect of the substitution pattern on water dynamics has precluded pinpointing the actual substituent effect.

To isolate the effects of individual methyl groups on the water dynamics and to explore the relation to the denaturation tendency, we herein report on water's hydrogen bond strength distribution, its fluctuation, and molecular rotation dynamics in solutions of 1-methylurea (1-MU) using a combination of linear and non-linear infrared (IR) spectroscopies. Our results show that introducing a single methyl group onto the urea scaffold already slows down the picosecond water hydrogen bond dynamics. A comparison to our earlier results shows that further methylation does not necessarily lead to further retardation of water dynamics.

EXPERIMENTAL SECTION

1-methylurea ($\geq 98\%$) was purchased from TCI chemicals, Germany, and used without further purification. Solutions were prepared by weight in 4% D_2O (99.9% D, Sigma-Aldrich)— H_2O (MilliQ) mixtures and sonicated for 30 min to ensure complete dissolution. Solute concentrations are reported in molality, $b(\mathbf{1-MU})$ [m]: moles of solute per kg of solvent.

To study hydrogen-bonding structure and dynamics, we perform infrared absorption, infrared pump-probe, and two-dimensional infrared spectroscopic experiments (for experimental details, see Ref. 9). Briefly, all experiments were performed in transmission on samples confined between 2 mm thick CaF_2 windows separated with 25–50 μm Teflon spacers. Linear infrared absorption spectra were recorded on a Nicolet Magna-IR 850 Series II Fourier-transform infrared (FTIR) spectrometer equipped with a DTGS detector. Polarization-resolved femtosecond IR pump-probe experiments were conducted using a home-built transient spectrometer.⁹ Broadband linearly polarized IR pulses (350 cm^{-1} FWHM, 200 fs, and 15 μJ) were tuned to be in resonance with the absorption maximum of $\nu(\text{OD})$ of HDO ($\sim 2500 \text{ cm}^{-1}$, 4 μm). We recorded changes in the absorption of a weak probe pulse, $\Delta\alpha$, which was induced by the interaction with a strong pump pulse (transient absorption). Absorption changes, both parallel, $\Delta\alpha_{\parallel}$, and perpendicular, $\Delta\alpha_{\perp}$, to the pump polarization as a function of the inter-pulse waiting time, T_w , were collected. The probe frequencies, $\tilde{\nu}_{\text{probe}}$, were resolved using a monochromator coupled with an HgCdTe array detector. From the measured data, we construct the isotropic signal, $\Delta\alpha_{\text{iso}}$, which is free of rotational contributions and only reflects population dynamics,³⁰

$$\Delta\alpha_{\text{iso}} = \frac{\Delta\alpha_{\parallel} + 2\Delta\alpha_{\perp}}{3}, \quad (1)$$

and the anisotropy parameter, R , which reports on the reorientation dynamics of the OD bond,³⁰

$$R = \frac{\Delta\alpha_{\parallel} - \Delta\alpha_{\perp}}{3\Delta\alpha_{\text{iso}}}. \quad (2)$$

Two dimensional IR (2D-IR) experiments were performed in pump-probe geometry^{31,32} using a commercial spectrometer (2DQuick from PhaseTech, Inc.). The pump frequency, $\tilde{\nu}_{\text{pump}}$, was resolved in the time domain by creating a pair of pump pulses with controlled relative phase and time delay using a pulse shaper based on a Ge acousto-optic modulator (AOM).^{31,32} The absorptive 2D-IR spectra reported here correspond to the parallel orientation of the pump and probe pulses.

RESULTS AND DISCUSSION

To study the effect of 1-MU on the hydrogen-bond strength distribution, we use the OD stretching vibration, $\nu(\text{OD})$, of HDO in water at $\sim 2500 \text{ cm}^{-1}$ as a spectroscopic probe of the water hydrogen bonding strength in solutions of 1-MU.^{9,33–36} Similar to other alkylureas,⁹ the addition of 1-MU hardly affects the center position and linewidth of the $\nu(\text{OD})$ band [Fig. 1(a)]—within experimental accuracy. At concentrations as high as 11 m, a low-frequency shoulder at $\sim 2450 \text{ cm}^{-1}$ emerges, which has been attributed to a solute vibration.^{9,28,37} Thus, the $\nu(\text{OD})$ infrared absorption band indicates that the average water hydrogen bonding strength distribution is not altered by 1-MU. Similar conclusions have been drawn from the $\nu(\text{OD})$ band for solutions of urea,^{28,29} although molecular dynamics simulations²⁹ suggest that for urea this insensitivity originates from a cancellation of minor spectral shifts due to somewhat weaker $\text{C}=\text{O} \cdots \text{water}$ hydrogen bonds and slightly enhanced $\text{water} \cdots \text{water}$ hydrogen-bonds.^{29,38} As such, the insensitivity of the $\nu(\text{OD})$ band implies that—similar to urea—also in the presence of 1-MU, both water–water hydrogen bonding in the solute's hydration shell and solute–water hydrogen bonds (e.g., with $\text{C}=\text{O}$ and/or $\text{N}-\text{H}$ groups of 1-MU) are of similar strength and comparable to the strengths of water–water hydrogen-bonds in bulk water.²⁹

To explore water's hydrogen-bonded structure in more detail, we study vibrational energy relaxation dynamics in solutions of 1-MU, which reports on vibrational energy transport and is, thus, sensitive to intermolecular coupling. The isotropic transient absorption data obtained from pump-probe experiments on the $\nu(\text{OD})$ vibration are shown in Fig. 1. In these experiments, a pump pulse promotes a fraction of $\nu(\text{OD})$ oscillators from the ground state $|0\rangle$ to the first vibrationally excited state $|1\rangle$. At short waiting times, the probe pulse reveals the reduced ground state population and the stimulated emission from the excited state, which appear as a negative (ground state bleach, GSB) contribution in the isotropic transient spectra $\Delta\alpha_{\text{iso}}$ around the $|0\rangle$ – $|1\rangle$ fundamental transition frequency. Simultaneously, the excited state absorption (ESA), which stems from $|1\rangle \rightarrow |2\rangle$ transitions, appears as a positive contribution shifted to lower frequencies due to the inherent anharmonicity of the $\nu(\text{OD})$ potential.³⁴ With increasing T_w , the excess vibrational energy is dissipated into the manifold of low-frequency modes, and the excited state population decays as reflected by the decay of these transient spectral signatures on a picosecond timescale. The finite transient signal at long waiting times reflects changes in the $\nu(\text{OD})$ absorption due to the population of the

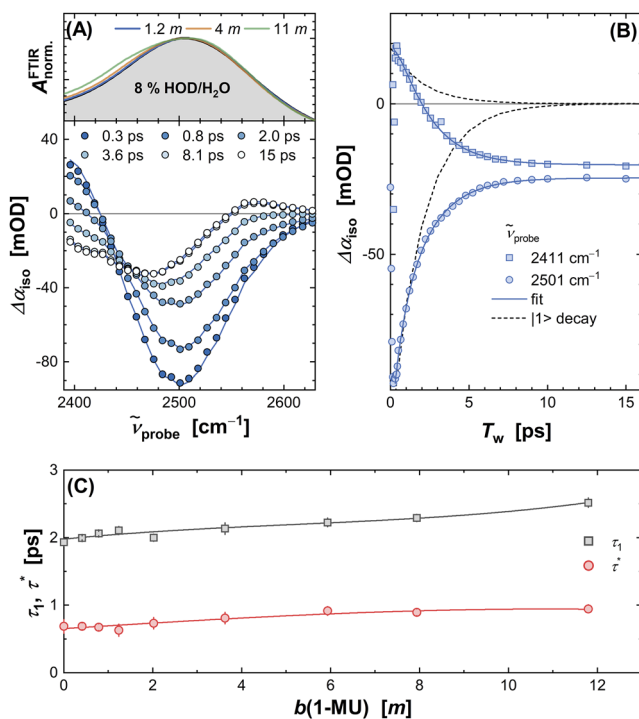


FIG. 1. (a) *Top panel:* Normalized linear FTIR spectra of $\nu(\text{OD})$ for solutions of 1-MU in 8% HOD in H_2O at selected concentrations. Gray-shaded area indicates the spectrum of 8% HOD in H_2O . *Bottom panel:* Isotropic transient spectra (symbols) for 1.2 m 1-MU at selected waiting times T_w . Lines are fits of the model described in the text to the data. (b) Isotropic transient signals as a function of waiting times T_w at selected $\tilde{\nu}_{\text{probe}}$. Solid lines show the fits using the cascade kinetic model. The black dashed lines show the decay of the excited state ($|1\rangle$) contribution. (c) Relaxation times obtained from fitting the kinetic model to the isotropic data at different concentrations of 1-MU. Error bars correspond to a 4% increase in the weighted sum of squared residuals of the fit. Lines are a guide to the eye.

low-frequency modes (“heated ground state”). We quantitatively describe these dynamics using a cascade kinetic model with two consecutive exponential relaxations, commonly found for the vibrational dynamics of the $\nu(\text{OD})$ band.^{34,39,40} In this model, the excited state population $|1\rangle$ decays to an intermediate state $|0'\rangle$ with a time constant τ_1 , which then decays to a thermalized ground state $|0^*\rangle$ with a time constant τ^* . The model provides an excellent description of the experimental data [Figs. 1(a) and 1(b)] over the entire probing frequency range at all concentrations studied here.

Both τ_1 and τ^* relaxation times moderately increase with the increasing concentration of 1-MU [Fig. 1(c)]. This slowdown can be attributed to the solute-induced effective truncation of the hydrogen-bonded network of water that serves as the bath for the dissipation of the excess vibrational energy. As such, complete dissipation of the excess energy and the concomitant structural relaxation of the solutions upon rising temperature⁴¹ are slowed down by 1-MU (see also discussion of the spectral diffusion dynamics below). We find the magnitude of the slow down for 1-MU in very close agreement with our previous report on alkylureas bearing two methyl(ene) groups⁹ as well as with earlier studies on tetramethylureas.^{33,35} Together with the observation that urea

has no appreciable effect on these dynamics,²⁸ our results suggest that a single methyl substituent at the urea scaffold leads to a noticeable slowdown of the vibrational energy flow, and additional methyl groups do not cause a further slowdown of these dynamics regardless of the substitution pattern.⁹

The energy relaxation dynamics, which require energy transfer to lower frequency modes, often display little sensitivity to hydration. Conversely, the rotational dynamics of water molecules, which require the breaking of an existing hydrogen bond and formation of an intermolecular bond to a different neighboring molecule, give direct insights into the availability of bonding partners in the close vicinity and, thus, to hydration structure.^{42,43} To study the effect of 1-MU on the rotational dynamics of water molecules, we followed the excitation anisotropy R of $\nu(\text{OD})$. The pump pulse preferentially interacts with oscillators whose transition dipole moment is parallel to the pump pulse polarization. This allows tagging an instantaneous orientational configuration of the HOD molecules. During an ~ 5 ps long time window, dictated by the vibrational lifetime of $\nu(\text{OD})$, it is possible to interrogate the orientational information by a probe pulse with controlled polarization.^{30,34} Due to the rotational motion of the water molecules, the orientational memory of the configuration labeled by the pump pulse is progressively lost, which can be traced by the decay of the excitation anisotropy parameter R as a function of waiting time T_w . To obtain the excitation anisotropy of the excited $\nu(\text{OD})$, we subtract the contributions of the thermalized ground state $|0^*\rangle$ to the data, as obtained from the kinetic model described above.

Upon adding 1-MU, the decay of the excitation anisotropy of $\nu(\text{OD})$ of HOD molecules slows down [Fig. 2(a)]. To quantify this slowdown, we perform a weighted fit to a two-state model previously applied to urea²⁸ and its alkylated derivatives.^{9,35,36,44} Thus, we model the observed anisotropy as an ensemble weighted average of the bulk-like and “slow” water fractions. The former is represented by an exponential decay of R with a time constant $\tau_{\text{bulk}} \approx 2.3 \pm 0.2$ ps,³⁴ whereas the latter is modeled as a constant offset,

$$R(T_w) = R_0 \left\{ e^{-T_w/\tau_{\text{bulk}}} (1 - f^s) + f^s \right\}, \quad (3)$$

where R_0 is the anisotropy value at zero waiting time and f^s the fraction of water molecules with rotational dynamics much slower than bulk-like water. This approach implies that the characteristic time scale of the “slow” water dynamics is beyond the accessible time window of our experiments. We note that despite other models have been proposed to account for the exact degree of retardation,^{45–48} the present model provides an excellent description of the data with a minimum number of adjustable parameters,⁹ and the derived parameters can be directly compared to previous reports using the same model.^{9,28,35}

As can be seen from Fig. 2(b), the fraction of water with perturbed dynamics f^s rises steeply up to ~ 2 m and somewhat levels off at higher concentrations, similar to what has been found for other alkylureas.^{3,7,9,36,44} To relate these slowed down water fractions of water to the number of solute molecules, we calculate the apparent hydration numbers Z^{app} ,

$$Z^{\text{app}} = \frac{f^s}{bM}, \quad (4)$$

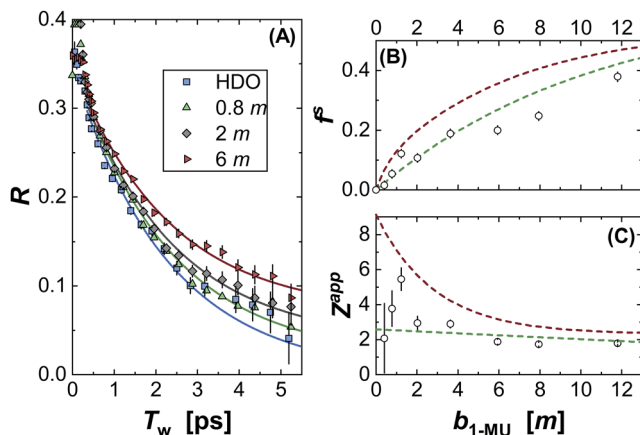


FIG. 2. (a) Excitation anisotropy decay of $\nu(\text{OD})$ for solutions of 1-MU in 8% HOD in H_2O at selected concentrations. The data (symbols) correspond to the weighted average around the center of the bleach ($\pm 10 \text{ cm}^{-1}$) after correcting for the heated ground state contribution.³⁴ Error bars are based on error propagation of the shot-to-shot standard deviation of the transient signals. Solid lines are fits using Eq. (3) to the data starting from $T_w \approx 350 \text{ fs}$ to avoid contributions due to fast librational dynamics, pulse overlap artifacts,³¹ or resonant energy transfer.⁴⁹ (b) Fraction of water molecules, f^s , with non-bulk rotational dynamics as a function of 1-MU molality (symbols). (c) Apparent hydration numbers, Z^{app} , corresponding to the number of water molecules with perturbed dynamics per one solute molecule (symbols). In panels (b) and (c), green dashed lines and red dashed lines show results for 1-EU and 1,3-DMU, respectively, taken from Ref. 9. Error bars in (b) and (c) are based on uncertainties of the fits of Eq. (3) to the anisotropy decay. Given that these errors do not account for co-variances of parameters or systematic errors, they may underestimate the uncertainty, in particular for Z^{app} at low concentrations.

where M is the molecular mass of water. The number of slowed-down water molecules per solute for 1-MU is similar ($Z^{\text{app}} \approx 2$) to that of 1,3-DMU and 1-EU at high solute concentrations [Fig. 2(c)], where hydration shells overlap.^{3,7,9,36} At low concentrations, we find ~ 3 water molecules perturbed per 1-MU molecule ($Z^{\text{app}} \approx 3$), which is similar to 1-EU and significantly lower than for 1,3-DMU [Fig. 2(c)]. Hence, our results suggest that 1-MU and 1-EU perturb water's rotational dynamics at low solute concentrations to a similar extent. The length of the substituting alkyl chain has only a minor effect. Conversely, the perturbation is enhanced by a second methyl group at the spatially separated nitrogen of urea in 1,3-DMU, consistent with the notion that the substitution pattern markedly affects the slowdown of water's rotation.^{2,9}

In order to gain insight into the hydrogen-bond strengthening/weakening dynamics, which do not necessarily lead to successful acceptor switches,⁵⁰ we performed two-dimensional IR spectroscopy (2D-IR).³¹ This method provides a time-resolved correlation of the pump and probe frequencies, which allows following the dynamics of the local microenvironments encountered by the vibrational probe. In water and aqueous solutions, this correlation is strong at short waiting times as the molecules retain their memory of the initial excitation frequency (hydrogen-bond strength); that is the $\nu(\text{OD})$ band is inhomogeneously broadened. In the 2D-spectra [left panel in Fig. 3(a)], this is manifested in the elongation of the signals along the diagonal line ($\tilde{\nu}_{\text{probe}} = \tilde{\nu}_{\text{pump}}$). Yet, the correlation

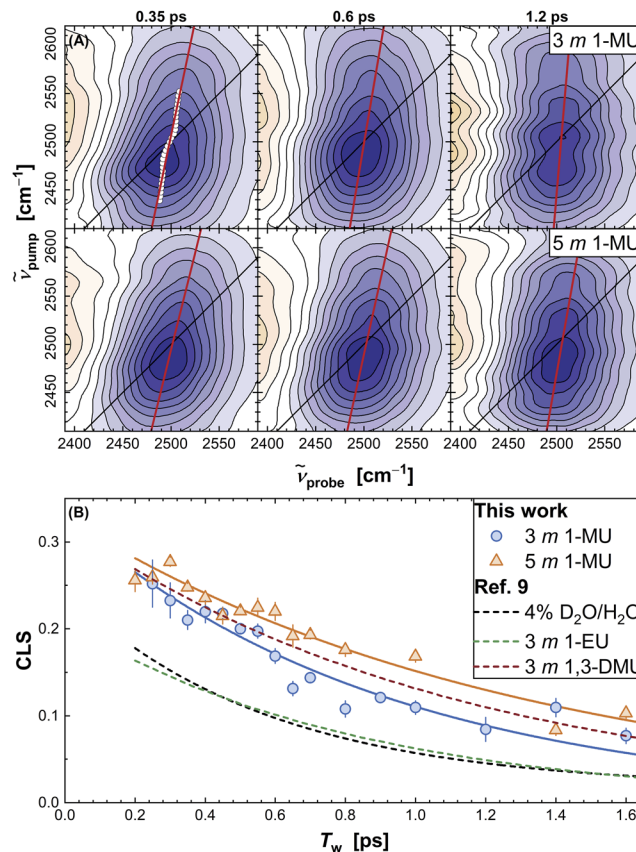


FIG. 3. (a) 2D-IR spectra at $\nu(\text{OD})$ frequencies for solutions of 3 m (top row) and 5 m (bottom row) 1-MU in 8% HOD in H_2O at selected waiting times T_w . Negative signals originating from $|0\rangle \rightarrow |1\rangle$ transitions are shown in shades of blue, and positive signals due to $|1\rangle \rightarrow |2\rangle$ transitions are shown in shades of orange. All spectra are normalized to the corresponding maximum bleaching signal. Contour lines represent increments by 10%. White symbols exemplarily show the centerline points. Solid red lines show the linear fits to the centerline points to determine the center line slope (CLS) values. (b) CLS values as a function of waiting time T_w (symbols). The error bars are uncertainties of the linear fits. Solid lines are single exponential fits with time constants of $0.9 \pm 0.1 \text{ ps}$ (3 m) and $1.3 \pm 0.1 \text{ ps}$ (5 m), whereas the dashed lines are the fits for neat solvent 4% $\text{D}_2\text{O}/\text{H}_2\text{O}$, 3 m 1,3-DMU, and 3 m 1-EU taken from Ref. 9.

quickly vanishes due to ultrafast fluctuations of the hydrogen bonding environment, which go along with the randomization of the instantaneous frequency of $\nu(\text{OD})$.^{31,37,51} We quantify these (spectral diffusion) dynamics using the center line slope (CLS) method^{31,51} by following the probe frequency of the minima of the $|0\rangle \rightarrow |1\rangle$ (bleaching) signal as a function of the pump frequency [white symbols in Fig. 3(a)]. The CLS corresponds to the slopes of the linear fits [red lines in Fig. 3(a)] to these minima. The thus obtained CLS values as a function of waiting time for 3 m and 5 m solutions of 1-MU are displayed in Fig. 3(b).

As already apparent from the 2D-IR spectra in Fig. 3(a) and quantitatively compared in Fig. 3(b), we find an enhanced initial (within the time resolution of our experiment) inhomogeneity of the microenvironments sampled by $\nu(\text{OD})$ for 3 m 1-MU as

compared to neat water,⁹ as evident from higher CLS values at short T_w . This heterogeneity increases further for 5 m 1-MU. Also, the decay of the CLS slows down with the increasing concentration of 1-MU [Fig. 3(b)], which can be traced to an increased hydrogen-bond lifetime and, hence, slower exchange of the water-solute hydrogen bonds, as suggested by MD simulations of solutions of other alkylureas.^{3,7,50} We have found a similar slowdown of water's hydrogen-bond dynamics for solutions of 1,3-DMU (and 1,1-DMU)⁹ and comparable dynamics have been reported for solutions of urea,²⁹ which has led us to conclude that hydrogen-bonding to the solutes' hydrogen bonding moieties (C=O and N-H) is the predominant cause for the observed slowdown of the water dynamics.⁹ In turn, the hydrogen-bonding heterogeneity and slowdown of hydrogen-bonding dynamics for 1-MU are more pronounced than for 1-EU [Fig. 3(b)], suggesting that the urea moiety of 1-MU is more exposed to water as compared to 1-EU. Our results, thus, indicate that the single methyl substituent does not make 1-MU sufficiently hydrophobic so that self-aggregation can reduce exposure of the hydrophilic urea group to the solvent, as opposed to 1-EU. Indeed, from protein denaturation studies¹⁷ using ureas substituted with linear alkyl groups, hydrophobic interactions have been reported to become significant for 1-EU and become increasingly important for ureas substituted with longer alkyl chains, resulting in stronger denaturation efficiency of 1-EU as compared to urea and methylated ureas.¹⁷ Given that solvent density fluctuations play an important role in the solvation of macromolecules,⁵² the similar hydrogen-bonded dynamics of solutions of methylated ureas—in contrast to 1-EU—may reflect this transition in the interaction motifs that underlie protein denaturation.

CONCLUDING REMARKS

In summary, using a combination of linear and non-linear infrared spectroscopies, we have shown that 1-MU can induce a noticeable slowdown of the water vibrational energy relaxation, reorientation, and hydrogen bond fluctuation dynamics, despite its negligible effect on the overall water hydrogen bond strength. Our results suggest that—in contrast to the reported negligible effect of urea itself—the rotational dynamics of up to 3 water molecules in the hydration shell of 1-MU are perturbed. We find the effect of 1-MU on the rotational dynamics similar to our earlier results for 1,1-DMU and 1-EU, suggesting that alkylation at only one of urea's nitrogen atoms similarly impacts water dynamics in its hydration shell, irrespective of the number of methyl groups. Thus, a single methyl group suffices to slow down water dynamics in 1-MU's hydration shell.

The addition of 1-MU to water also makes the short-time hydrogen-bonding microenvironment more heterogeneous, and hydrogen-bond strength correlation dynamics are slowed down. This effect of 1-MU is, however, similar to what has been reported for urea²⁹ and other alkylureas, except for 1-EU.⁹ This similarity for urea and methyl ureas suggests that water hydrogen-bonded to the hydrophilic urea moiety exhibits slower dynamics and that these groups are similarly exposed to water for 1-MU and dimethylureas. Hence, urea, 1-MU, and dimethylureas share a similar exposure of the hydrogen-bonding groups to water and also have a similar denaturing ability toward biomolecules.^{14–16} Given the similar exposure

to water, these hydrophilic moieties are also available for interaction with proteins, which has been suggested to be the predominant cause for urea-induced protein destabilization.⁵³ Likewise, the exposure of (alkyl-) ureas hydrogen-bonding groups will also correlate with the overall hydrogen-bond donor numbers of the alkylurea water mixtures, relevant to solvation of hydrophilic protein residues.⁴ In this context, our results may help explain the similar effect of urea bearing up to two methyl groups on proteins.

ACKNOWLEDGMENTS

We would like to thank Mischa Bonn for fruitful discussion. B.A.M. thanks the Alexander von Humboldt Foundation for funding via a postdoctoral scholarship. This project received funding from the European Research Council (ERC) under the European Union's Horizon 2020 research and innovation program (Grant No. 714691). Support from the MaxWater program of the Max Planck Society is acknowledged.

AUTHOR DECLARATIONS

Conflict of Interest

The authors have no conflicts to disclose.

DATA AVAILABILITY

The data that support the findings of this study are available from the corresponding author upon reasonable request.

REFERENCES

- 1 D. Ben-Amotz, *Annu. Rev. Phys. Chem.* **67**, 617 (2016).
- 2 G. Stirnemann, F. Sterpone, and D. Laage, *J. Phys. Chem. B* **115**, 3254 (2011).
- 3 V. Agieienko, C. Hözl, D. Horinek, and R. Buchner, *J. Phys. Chem. B* **122**, 5972 (2018).
- 4 B. Ding, L. Yang, D. Mukherjee, J. Chen, Y. Gao, and F. Gai, *J. Phys. Chem. Lett.* **9**, 2933 (2018).
- 5 V. Conti Nibali, S. Pezzotti, F. Sebastiani, D. R. Galimberti, G. Schwaab, M. Heyden, M.-P. Gageot, and M. Havenith, *J. Phys. Chem. Lett.* **11**, 4809 (2020).
- 6 D. Ben-Amotz, *J. Am. Chem. Soc.* **141**, 10569 (2019).
- 7 V. Agieienko, D. Horinek, and R. Buchner, *Phys. Chem. Chem. Phys.* **19**, 219 (2017).
- 8 G. Della Gatta, E. Badae, M. Józwiak, and P. Del Vecchio, *J. Chem. Eng. Data* **52**, 419 (2007).
- 9 B. A. Marekha and J. Hunger, *Phys. Chem. Chem. Phys.* **21**, 20672 (2019).
- 10 U. Kaatzte, *J. Chem. Phys.* **148**, 014504 (2018).
- 11 U. Kaatzte and A. Rupperecht, *J. Chem. Phys.* **117**, 4936 (2002).
- 12 S. T. van der Post, K.-J. Tielrooij, J. Hunger, E. H. G. Backus, and H. J. Bakker, *Faraday Discuss.* **160**, 171 (2013).
- 13 X. Cheng, I. A. Shkel, K. O'Connor, J. Henrich, C. Molzahn, D. Lambert, and M. T. Record, *J. Am. Chem. Soc.* **139**, 9885 (2017).
- 14 N. Poklar, G. Vesnaver, and S. Lapanje, *J. Protein Chem.* **13**, 323 (1994).
- 15 N. Poklar, N. Petrovčič, M. Oblak, and G. Vesnaver, *Protein Sci.* **8**, 832 (2008).
- 16 T. T. Herskovits and H. Jaillet, *Science* **163**, 282 (1969).
- 17 T. T. Herskovits, H. Jaillet, and B. Gadegbeku, *J. Biol. Chem.* **245**, 4544 (1970).
- 18 L. B. Sagle, Y. Zhang, V. A. Litosh, X. Chen, Y. Cho, and P. S. Cremer, *J. Am. Chem. Soc.* **131**, 9304 (2009).
- 19 H. Wei, Y. Fan, and Y. Q. Gao, *J. Phys. Chem. B* **114**, 557 (2010).
- 20 U. Kaatzte, H. Gerke, and R. Pottel, *J. Phys. Chem.* **90**, 5464 (1986).

- ²¹J. Krakowiak and J. Wawer, *J. Chem. Thermodyn.* **79**, 109 (2014).
- ²²W. H. Brandeburgo, S. T. van der Post, E. J. Meijer, and B. Ensing, *Phys. Chem. Chem. Phys.* **17**, 24968 (2015).
- ²³J. Krakowiak, J. Wawer, and A. Panuszko, *J. Chem. Thermodyn.* **58**, 211 (2013).
- ²⁴G. Della Gatta, E. Badea, M. Józwiak, and G. Barone, *J. Chem. Eng. Data* **54**, 2739 (2009).
- ²⁵F. Perakis, L. De Marco, A. Shalit, F. Tang, Z. R. Kann, T. D. Kühne, R. Torre, M. Bonn, and Y. Nagata, *Chem. Rev.* **116**, 7590 (2016).
- ²⁶A. A. Bakulin, C. Liang, T. la Cour Jansen, D. A. Wiersma, H. J. Bakker, and M. S. Pshenichnikov, *Acc. Chem. Res.* **42**, 1229 (2009).
- ²⁷D. Laage, T. Elsaesser, and J. T. Hynes, *Chem. Rev.* **117**, 10694 (2017).
- ²⁸Y. L. A. Rezus and H. J. Bakker, *Proc. Natl. Acad. Sci. U. S. A.* **103**, 18417 (2006).
- ²⁹J. K. Carr, L. E. Buchanan, J. R. Schmidt, M. T. Zanni, and J. L. Skinner, *J. Phys. Chem. B* **117**, 13291 (2013).
- ³⁰H.-S. Tan, I. R. Piletic, and M. D. Fayer, *J. Opt. Soc. Am. B* **22**, 2009 (2005).
- ³¹P. Hamm and M. Zanni, *Concepts and Methods of 2D Infrared Spectroscopy* (Cambridge University Press, Oxford, UK, 2011).
- ³²S.-H. Shim and M. T. Zanni, *Phys. Chem. Chem. Phys.* **11**, 748 (2009).
- ³³Y. L. A. Rezus and H. J. Bakker, *J. Phys. Chem. A* **112**, 2355 (2008).
- ³⁴Y. L. A. Rezus and H. J. Bakker, *J. Chem. Phys.* **123**, 114502 (2005).
- ³⁵Y. L. A. Rezus and H. J. Bakker, *Phys. Rev. Lett.* **99**, 148301 (2007).
- ³⁶K.-J. Tielrooij, J. Hunger, R. Buchner, M. Bonn, and H. J. Bakker, *J. Am. Chem. Soc.* **132**, 15671 (2010).
- ³⁷C. Yan, P. L. Kramer, R. Yuan, and M. D. Fayer, *J. Am. Chem. Soc.* **140**, 9466 (2018).
- ³⁸M. C. Stumpe and H. Grubmüller, *J. Phys. Chem. B* **111**, 6220 (2007).
- ³⁹K. Mazur, M. Bonn, and J. Hunger, *J. Phys. Chem. B* **119**, 1558 (2015).
- ⁴⁰B. Ensing, A. Tiwari, M. Tros, J. Hunger, S. R. Domingos, C. Pérez, G. Smits, M. Bonn, D. Bonn, and S. Woutersen, *Nat. Commun.* **10**, 2893 (2019).
- ⁴¹Z.-P. Zheng, W. Fan, S. Roy, K. Mazur, A. Nazet, R. Buchner, M. Bonn, and J. Hunger, *Angew. Chem., Int. Ed.* **54**, 687 (2015).
- ⁴²D. Laage and J. T. Hynes, *J. Phys. Chem. B* **112**, 14230 (2008).
- ⁴³H. J. Bakker and J. L. Skinner, *Chem. Rev.* **110**, 1498 (2010).
- ⁴⁴A. A. Bakulin, M. S. Pshenichnikov, H. J. Bakker, and C. Petersen, *J. Phys. Chem. A* **115**, 1821 (2011).
- ⁴⁵G. Stirnemann, E. Wernersson, P. Jungwirth, and D. Laage, *J. Am. Chem. Soc.* **135**, 11824 (2013).
- ⁴⁶G. Stirnemann, J. T. Hynes, and D. Laage, *J. Phys. Chem. B* **114**, 3052 (2010).
- ⁴⁷D. Laage, G. Stirnemann, F. Sterpone, R. Rey, and J. T. Hynes, *Annu. Rev. Phys. Chem.* **62**, 395 (2011).
- ⁴⁸J. Qvist and B. Halle, *J. Am. Chem. Soc.* **130**, 10345 (2008).
- ⁴⁹L. Piatkowski, K. B. Eisenthal, and H. J. Bakker, *Phys. Chem. Chem. Phys.* **11**, 9033 (2009).
- ⁵⁰D. Laage, G. Stirnemann, and J. T. Hynes, *J. Photochem. Photobiol., A* **234**, 75 (2012).
- ⁵¹E. E. Fenn and M. D. Fayer, *J. Chem. Phys.* **135**, 074502 (2011).
- ⁵²N. F. A. van der Vegt, *J. Phys. Chem. B* **125**, 5191 (2021).
- ⁵³D. R. Canchi and A. E. García, *Annu. Rev. Phys. Chem.* **64**, 273 (2013).